LARGE ORBIT GYROKLYSTRON DEVELOPMENT AT LOS ALAMOS

R. M. Stringfield, R. M. Wheat, D. J. Brown, M. V. Fazio, J. Kinross-Wright, B. E. Carlsten, G. Rodenz, R. J. Faehl, R. F. Hoeberling
Los Alamos National Laboratory, Los Alamos, New Mexico, 87545

Abstract

We have designed and are testing a large orbit gyroklystron amplifier for 1.3 GHz operation in 65 ns pulses. The ultimate power output goal is 500 MW with a gain in excess of 20 dB. This initial investigation is intended to lay the groundwork for operation at 11.4 GHz for particle accelerator applications, and also at frequencies of up to 35 GHz for other uses. Computational design has been performed with the resonant cavity code MAFIA and the particle in cell codes MERLIN and ISIS. Electron beam optics through a magnetic cusp was also studied with ISIS and MERLIN, and verified experimentally, to develop a suitable electron beam trajectory from the diode into the resonator region. Performance tests of a single stage device have been performed. An unsaturated gain of 43 dB has been observeed using 4 kW of input drive, yielding an amplified output of 100 MW.

Introduction

A large orbit gyrotron (gyroklystron) (LOG) amplifier operating at 1.3 GHz is being developed to operate at powers of up to 500 MW for 65 ns pulses. While this initial investigation is being performed at 1.3 GHz, this device can be scaled to higher frequencies in a straight forward fashion. LOG oscillators have operated at 15 GHz and higher frequencies with comparable performance to that at lower frequencies. Amplifier operation has been examined theoretically and experimentally, but less extensively [1-4].

These devices produce microwaves by the interaction of a helically rotating electron beam with the oscillating fields of a resonant cavity structure. The beam is formed by injecting a hollow, non-rotating beam, born in an axial magnetic field, through a magnetic cusp positioned at the anode plane. An annular slot is cut into the mild steel cusp plate to allow the beam to pass into the downstream resonator. In the cusp, a portion of the axial beam energy is converted to rotational energy. Typical ratios of rotational velocity to axial velocity (defined as alpha) are in the range of 1.5 to 2.5. The electron beam entering the resonator has an energy of 500-700 keV, a current of 1-3 kA, and a radius of 5-8 cm. The device, shown in Figure 1, employs a cylindrical resonator with three vanes in the wall spaced equally in azimuth.

The amplifier is designed as two resonator device, with cylindrical resonators of the type describe above. The vane structure is used to evoke coupling of the rotating electron beam with the TE(0,1,n) resonant cavity mode of the cylindrical structure by modifying the normally circular electric field pattern of the mode into a scalloped pattern, similar to the TE(3,1,n) mode, but near the lower TE(0,1,n) resonant frequency for a non-vaned cylindrical wall with an intermediate radius.

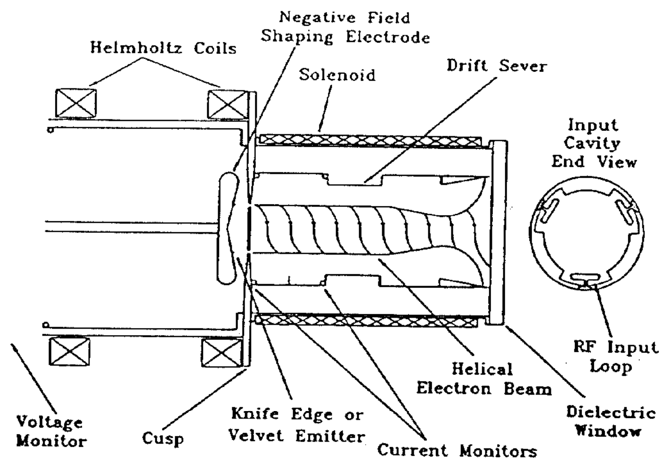

Figure 1. Large orbit gyrotron and gyroklystron geometry. Two resonator stages are shown, although single stage operation also will be investigated.

Rf is fed into the cavity using two loops, one in each of two of the vanes at the axial midplane. The standing wave pattern of the cavity will couple to the rotating beam, provided the beam angular velocity is in synchronism, in such a way that an azimuthal density perturbation will grow on the beam with three density maxima around the azimuth. The magnitude of the density variation will grow as the beam propagates down the length of the resonator, influenced both by the applied oscillating fields, and the space charge self fields of the beam that drive the negative mass instability. The instability will grow as the electron beam propagates through the system. Feedback from the beam instability drives the cavity fields to greater amplitude.

The downstream end of the first cavity has a central opening which forms the entrance to a cylindrical, non-vaned electron beam drift pipe. The pipe is intended to serve the role of an rf isolating sever between the first and second cavities, and also as a region in which the beam bunching can grow by the negative mass instability, independent of applied microwave fields. An optimum drift pipe length will be determined experimentally to maximize azimuthal beam bunching. A second, output resonator designed to be strongly coupled to the beam will be place downstream of the drift pipe at the point of optimum beam bunching to extract rf energy.

Both 2.5 D particle in cell modeling with the code ISIS was used to design the electron gun, and subsequent experiments were performed that correlated well to the computer design. The electron beam from this design is an annulus 0.5 to 1.0 cm thick, at a radius of 7.1 cm, at an energy of 650 kV, a current of 2 to 3 kA, and an alpha ranging from 1.5 to 2.5, depending upon the magnetic field strength, that ranged

0-7803-1203-1/93$03.00 © 1993 IEEE

from 300 to 500 G. More detail of the design of the electron beam is contained in a previous paper[5].

Experimental Studies

The experimental configuration consists of the diode, cusp and magnetic field coils, downstream resonator section, and a dielectric vacuum window for radiating the microwaves into an anechoic volume downstream of the vacuum chamber. A 4 kW 1.3 GHz source provides rf input drive to the resonator in these initial studies. Up to 20 MW is available as input drive but will require device modifications for aperture coupling to accommodate the power. Presently, magnetic loops are situated at the base of two of the vanes for cavity input drive. A loop in the third vane is used to monitor the standing wave field in the cavity. A stub waveguide receiver is positioned in the anechoic volume downstream of the open resonator end to monitor the radiated power in the far field.

We evaluate amplifier performance by comparing the radiated microwave power in three different circumstances. First, the radiated power due to the 4 kW input drive alone is measured. Second, the radiated power with no input drive, but with the electron beam injected, is measured. Finally, the radiated power when both input rf drive and injected electron beam are present in the resonator is measured. Relative power measurements among shots are performed by comparing detected signals received with a waveguide stub placed at a fixed location in the far field downstream of the open ended resonator.

Two significant operating regimes using the single resonator were found. The first regime, operated at a higher ratio of magnetic field to beam voltage (330 gauss/775 kV), appears to be attractive for the two stage gyroklystron (Figure 1) to establish an initiating beam modulation in a first cavity. This ratio is an experimental analog to B/γ, the crucial parameter governing the cyclotron frequency of the rotating beam. The initial bunching in the first cavity would be allowed to grow as the beam drifts to the second cavity. This operating regime showed significant rf production both with and without rf input drive, indicating a tendency for the device to oscillate. However, when rf input drive was present, improvements in the pulse length of the detected rf power signals, pulse energy, frequency purity of the fast Fourier transforms, and the shot to shot statistical consistency were observed. For example, this operating regime yielded rf pulse lengths of only 42 ns when the input drive was off. This effect represents a 55 percent increase in pulse length due to the presence of rf input drive. Table 1 summarizes these results. Figure 2 depicts typical detected power and downconverted mixer signals for the cases of no input drive and 4 kW of input drive.

The second operating regime appears to be most applicable to a single stage amplifier. It uses a slightly lower ratio of magnetic field to voltage (340 gauss/850 kV). In this case we saw a significant increase in output power and energy using input rf drive of 4 kW, compared with the output when no input rf was used. While final output power determinations have not yet been completed, approximately 100 (+/- 3 dB) MW of additional power is produced from the device when 4 kW of input drive is used. This corresponds to an amplifier gain in excess of 40 dB. The frequency purity as indicated by the FFT shows the amplified bandwidth to be 25 percent narrower than

RF Input Drive Power (4 kW) ON, Sample Size = 8

	Stub Horn (W)	Duration (ns)	RF Energy (arb)	FFT Freq (MHz)	FFT FWHM (MHz)
Mean	5450	60	3.27	1285	27
Std. Dev.	729	16	0.98	2.5	17

Input Drive Power OFF, Sample Size = 17

	Stub Horn (W)	Duration (ns)	RF Energy (arb)	FFT Freq (MHz)	FFT FWHM (MHz)
Mean	7406	42	3.11	1284	36
Std. Dev.	2089	24	1.98	2.9	25

Table 1. Mean values and standard deviations for several performance characteristics comparing the cases of rf input drive on and off for magnetic field strength and beam voltage of 330 G and 775 kV. Listed are stub horn power amplitude (watts), rf power pulse duration (ns), time integrated rf energy (arbitrary units), and fast Fourier transform (FFT) frequency spectra.

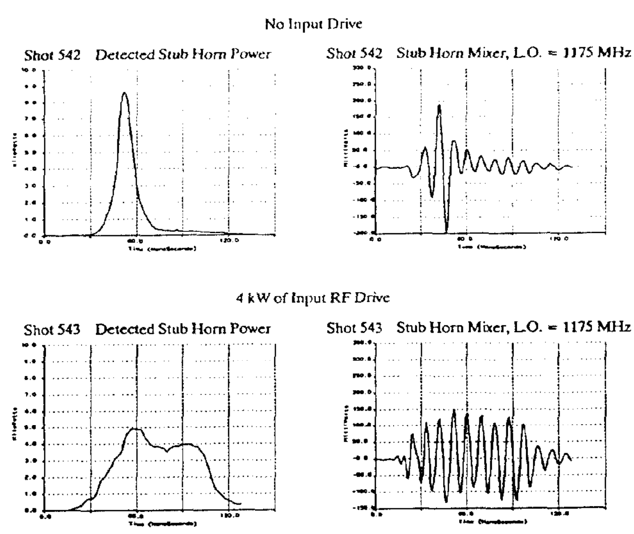

Figure 2. Typical detected diode power and downconverted mixer signals for the cases of Table 1. Stub horn power is 10 kW full scale. The FFT scale is arbitrary, and the same for both cases. The time scale is 20 ns/div.

the bandwidth without input drive (2.0% vs 2.5%), suggesting that the bandwidth is approaching but not quite at the Fourier limit, growing narrower with longer pulse length. Saturated gain has not yet been measured due to temporary difficulty in connecting a more powerful input drive source to the experiment. Hence, device efficiency as a percentage of electron beam power has not been determined. Table 2 lists the operating conditions which yielded significant power gain in the single resonator amplifier. Figure 3 depicts representative detected power and downconverted mixer signals for the two cases. Using the method described above for estimating amplifier output power from the stub horn power (9807 W) the total power radiated was 157 MW.

Summary

The study and construction of a large orbit gyrotron and two stage gyroklystron amplifier are underway. Modeling and experiments have been performed to design these devices. Experiments are ongoing to measure and optimize the performance of the single stage device, in preparation for subsequent two stage operation. Improvements in the quality of the rf output pulse produce by the first (rf input) cavity of the device have been found as the result of injecting input rf power into the cavity. This work has been supported by the Los Alamos National Laboratory Independent Research and Development Program, sponsored by the U. S. Department of Energy.

RF Input Drive Power (4 kW) ON, Sample Size = 14

	Stub Horn (W)	Duration (ns)	RF Energy (arb)	FFT Freq (MHz)	FFT FWHM (MHz)
Mean	9807	42.7	2.69	1280	44.1
Std. Dev.	5318	13.3	1.78	14.7	37.9

Input Drive Power OFF, Sample Size = 14

	Stub Horn (W)	Duration (ns)	RF Energy (arb)	FFT Freq (MHz)	FFT FWHM (MHz)
Mean	3060	22.3	0.67	1286	78.8
Std. Dev.	2027	19.1	0.45	17.5	37.9

Table 2. Mean values and standard deviations for several performance characteristics comparing the cases of rf input drive on and off for magnetic field strength and beam voltage of 340 G and 850 kV. This case shows clear amplification from a single stage device.

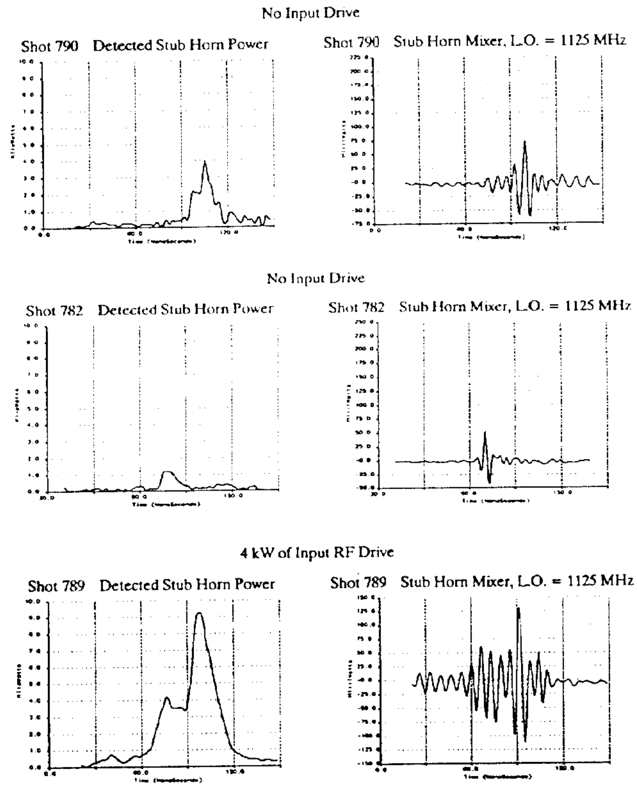

Figure 3. Typical detected power and downconverted mixer signals for the cases of Table 2. Two shots without input drive are shown to indicate the upper and lower limits of self oscillation with no drive power. Stub horn power is 10 kW full scale. The FFT scale is arbitrary, and the same for both cases. The time scale is 20 ns/div.

1. W. W. Destler, et al, "High-power microwave generation from large-orbit devices," IEEE Trans. on Plasma Science **PS-16** (2), April 1988, p71.
2. Y. Y. Lau and L. R. Barnett, "Theory of a low magnetic field gyrotron (gyromagnetron)," Int. J. of Infrared and Millimeter Waves 3 (5), 1982, p. 619.
3. J. Y. Choe, K. Boulais, V. Ayres, W. Namkung, and H. Uhm, "Preliminary study of cusptron amplifier," Microwave and Particle Beam Sources and Directed Energy Concepts, SPIE **1061** (1989) p. 132.
4. K. R. Chu, et al, "Theory, design, and operation of large-orbit high harmonic gyroklystron amplifiers," IEEE Trans. on Plasma Science **PS-13** (6), December 1985, p 435.
5. R. Stringfield, et al, "Large Orbit Gyroklystron Development at Los Alamos," Proc. 1992 Linear Accelerator Conf., Ottawa, Ontario, Canada, August 1992, AECL-10728, Vol. p. 190-192